Hysteresis phenomena in distributed optical systems

N. N. Rozanov

(Submitted 31 May 1980)
Zh. Eksp. Teor. Fiz. 80, 96–108 (January 1981)

Distinguishing features of hysteresis in distributed systems are demonstrated by using as examples two nonlinear-optics problems, optical thermal breakdown of semiconductors, and optical bistability in a nonlinear interferometer. The existence of waves due to switching between states corresponding to different branches of the hysteresis loop is demonstrated, as well as the presence of boundary layers and of hysteresis of the transverse profile of the output parameters at fixed input parameters. The hysteresis changes do not occur simultaneously over the entire cross section of the incident beam, but only in a narrow zone which is at the front of the switching wave. This front moves in a transverse direction at a velocity that vanishes when a definite position that corresponds to the quasistationary boundary layer is approached.

PACS numbers: 42.65. — k

Hysteresis changes in nonlinear mechanical, electric and other lumped systems have by now been well investigated. Typical examples are the oscillations of a nonlinear oscillator under the influence of a periodic force, and hard excitation of oscillations.[1] Hysteresis of the same type takes place in competition between laser modes[2,3] and in lasers with nonlinear cells.[4] Advances in nonlinear optics have led to the observation of many related hysteresis phenomena when laser radiation acts on passive objects. These include the hysteresis produced when electromagnetic radiation is reflected from nonlinear media and layers,[5-12] in optical thermal breakdown of semiconductors,[13] and in interferometers filled with nonlinear media (see the review by Lugovoĭ[14]).

The indicated phenomena, particularly nonlinear interferometers, can have important applications, as indicated already in Ref. 15. At the same time, they possess a number of interesting physical features. In recent years, in addition to the increase in the number of nonlinear effects that lead to hysteresis,[16-18] intensive studies have been made of fluctuations and statistics of phonons and of the relation between optical hysteresis and phase transitions.[18-23] We shall be interested here in nonlinear optical systems that are not lumped but distributed, and have an infinite number of degrees of freedom. In the previously employed theoretical analysis the system was assumed to be lumped. In fact, in the most widely used approximation, that of a plane incident wave, all the points of the beam cross section are assumed identical and in the general case hysteresis cannot be described for a bounded light beam. Another approach, based on mode expansion in a resonator with a nonlinear medium, is suitable in principle for the analysis of hysteresis of a distributed system if an infinite number of modes is considered. In its actual application, however, which is feasible only for a small number of modes, the problem reduces to the analysis of one or several interacting nonlinear oscillators,[14] i.e., again to a lumped system. Such a substitution presupposes the introduction into the nonlinear resonator of several special filters, which are absent in most experiments. That the analysis of nonlinear interferometers with the aid of modes having a fixed transverse structure is inadequate was likewise noted in Lugovoĭ's review.[14]

We consider in this paper hysteresis effects connected with "the transverse distributivity" of bistable optical systems. (Manifestations of "longitudinal distributivity" are discussed in the Conclusion.) Optical bistability is understood here in a broad sense. Its definitive attribute is an S-shaped[1)] plot of the output characteristics (e.g., the power of the outgoing or reflected radiation, or else a parameter of the state of the nonlinear system) against the optical power in the quasistationary regime. An ambiguous dependence of this kind is obtained in the plane-wave approximation for all the systems indicated above, with the middle branch unstable.

If an optical beam is broad enough, diffraction effects are weakly pronounced. It would then be possible, using geometric optics, to break up the beam into individual light tubes, within each of which the use of the plane-wave approximation would make it possible to determine the corresponding local output parameter.[24] This approach leads to a satisfactory solution of the problem, but only in the absence of hysteresis, when the considered dependence of the output characteristics on the input characteristic is single-valued. Indeed, in the case of an S-shaped characteristic the central part of an incident beam of sufficient intensity will correspond to the upper branch of the S-shaped curve, whereas the peripheral part will correspond to the lower branch (see Fig. 3 below). The geometric-optics approximation does not permit matching of the solutions corresponding to the upper and lower branches. Of fundamental importance here is the allowance for even weak interaction of the light cubes. This circumstance was pointed out in our paper[25] in connection with a discussion of the role of the spatial limits of an incident beam in hysteresis effects when light is reflected from a nonlinear medium.[26] A numerical analysis relating to nonlinear interferometers[27] confirms the point of view advanced in Ref. 25.

In the present paper, using two nonlinear distributed systems as the example, we construct analytically the transverse profiles of the output parameter, demonstrate the existence, under certain conditions, of a boundary layer in which the output parameter has an anomalously abrupt variation, and obtain the hystere-

 0038-5646/81/010047-07$02.40

sis of the transverse profiles and its kinetics. The similarity of the results obtained for systems that are substantially different physically, as well as the presence of related phenomena for waves in chemical and biological kinetics[28-31] and in switching effects in plasma and in solids,[32] indicate that all exhibit rather common features of hysteresis of distributed systems.

1. OPTICAL THERMAL BREAKDOWN OF SEMICONDUCTORS

A convenient example with which to demonstrate the specific features of hysteresis of a distributed system is the temperature profile $T(x)$ in a thin semiconducting rod, whose lateral face is irradiated by a broad light beam of intensity $G(x)$, where x is the coordinate along the rod axis.[33] The temperature dependence of the light-absorption coefficient $\alpha(T)$ can be arbitrary. In a case typical of semiconductors (see Ref. 12) it can be assumed, for example, that

$$\alpha(T)=\alpha_\infty \exp(-E_g/2kT), \tag{1.1}$$

where E_g is the gap width, k is Boltzmann's constant, and $\alpha_\infty=\text{const}$ is the value of the absorption coefficient at high temperatures.

The heat conduction equation for a temperature averaged over the rod cross section is

$$c\frac{\partial T}{\partial t}=\lambda\frac{\partial^2 T}{\partial x^2}+G(x,t)P(T)-H(T-T_0). \tag{1.2}$$

Here c is the bulk specific heat, λ and H are the coefficients of thermal conductivity and heat transfer, T_0 is the ambient temperature, and P is the per-unit absorption averaged over the path length l in the rod:

$$P(T)=[1-e^{-\alpha(T)l}]/l.$$

We change to dimensionless quantities

$$\theta=T/T_0,\quad X=x/x_0,\quad w=G\alpha_0/HT_0,$$
$$\mu=\lambda/Hx_0^2,\quad a(\theta)=P/\alpha_0,\quad b(\theta)=\theta-1, \tag{1.3}$$

where x_0 and α_0 are the characteristic values of the light-beam width and of the absorption coefficient. Taking (1.3) into account, we obtain for stationary regimes

$$\mu d^2\theta/dX^2=F,\quad F=-w(X)a(\theta)+b(\theta). \tag{1.4}$$

We assume that the rod length exceeds greatly the beam width, so that the boundary conditions can be written in the form[2)]

$$d\theta/dX|_{X\to\pm\infty}=0. \tag{1.5}$$

To solve the problem (1.4), (1.5) it is useful to resort to a mechanical analogy (see, e.g., Refs. 5 and 9). We can regard (1.4) as Newton's equation for the motion of a particle of mass μ under the influence of a force F. The corresponding "potential energy" is

$$U=wA(\theta)-B(\theta), \tag{1.6}$$

$$A(\theta)=\int_0^\theta a(\theta)d\theta,\quad B(\theta)=\int^\theta b(\theta)d\theta=\frac{1}{2}(\theta-1)^2+\text{const}.$$

If we assume (1.1), then at $\alpha_\infty l\ll 1$, $\alpha_0=\alpha_\infty$, and $\xi=2kT_0/E_g$ we have

$$A(\theta)=\xi^{-1}[\mathrm{Ei}(-1/\xi\theta)+\xi\theta\exp(-1/\xi\theta)], \tag{1.7}$$

where Ei is the integral exponential function. We introduce the "energy" E

$$E={}^1/_2\mu(d\theta/dX)^2+U. \tag{1.8}$$

It follows from (1.4) that

$$dE/dX=A(\theta)dw/dX.$$

Therefore on the rising sections of $w(X)$ the energy E increases at a rate proportional to the rate of transverse change of the intensity of the incident beam. If $w(X)$ is constant on some interval[3)] then E is constant and

$$X=\pm\left(\frac{\mu}{2}\right)^{1/2}\int^\theta\frac{d\theta}{[E-U(\theta)]^{1/2}}+\text{const}. \tag{1.9}$$

The determination of the temperature distribution $\theta(X)$ at constant $w(X)$ reduces thus to a solution of the classical problem of one-dimensional motion in a potential field.[34] According to (1.6), the potential U is a linear function of the light intensity w with a slope $A(\theta)>0$. The situation typical of hysteresis conditions is illustrated in Fig. 1. The potential curves have single humps at $w>w_1$ and $w<w_2$ and two humps at $w_2<w>w_1$; the left hump is higher than the right one if $w_2<w<w_t$ and lower if $w_t<w<w_1$. The extrema of the potential curves correspond to homogeneous (independent of the coordinate X) solutions of (1.4), (1.5), for which $F=0$ and

$$a(\theta)=b(\theta)/w. \tag{1.10}$$

A graphic interpretation of (1.10) is shown in Fig. 2. The points of intersection of the lower branch of the $a(\theta)$ curve with the lines $b(\theta)/w$ ($w<w_1$) corresponds to the line LL, which joins on Fig. 1 the vertices of the left-hand humps, and also to the lower branch of the hysteresis curve of Fig. 3b. Analogously, the points of intersection of the upper branch of the $a(\theta)$ curve with the line ($w>w2$) corresponds to the line RR (Fig. 1) that passes through the vertices of the upper humps, and to the upper branch of the hystersis curve in Fig. 3b. Hysteresis is possible, generally speaking, in the range $w_2<w<w_1$. [In the case corresponding to (1.7), a necessary condition for hysteresis is $\xi<\frac{1}{4}$]. The stability of the homogeneous solutions is determined in

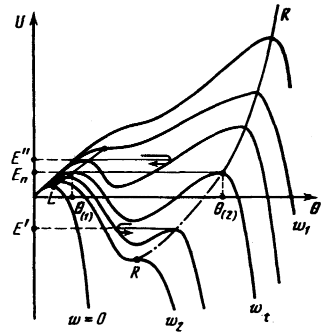

FIG. 1. "Potential curves" U for different intensities of the incident radiation. The trajectories with "energies" E' and E'' are the temperature profiles for the inhomogeneous solutions while E_t and w_t correspond to the boundary layer that "matches" the left and right humps of different heights.

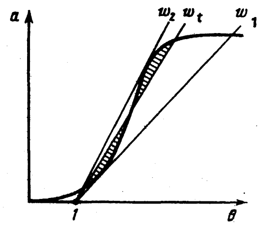

FIG. 2. Typical plot of a (θ). The intensities $w = w_t$ correspond to equality of the two shaded areas.

standard fashion by invoking the nonstationary equation

$$-\frac{\partial\theta}{\partial\tau}+\mu\frac{\partial^2\theta}{\partial X^2}=F(\theta), \tag{1.11}$$

where $\tau = tH/c$ is the dimensionless time. It is easily seen that the growth rate of small perturbations is proportional to the curvature of the potential curve $d^2U/d\theta^2$ in the corresponding extremum. Therefore the intermediate branch of the hysteresis curve is unstable, whereas the upper and lower branches are stable.

In the intensity interval $w_2 < w < w_1$, in addition to the invariant temperature profiles with constant θ, there are also inhomogeneous (X-dependent) stationary solutions of the problem (1.4), (1.5) (Fig. 1, the trajectories $E = E'$ and $E = E''$ [4]). The corresponding temperature dependence $\theta(X)$ has in a certain "central" region either a minimum ($w < w_t$, $E = E'$) or a maximum ($w > w_t$, $E = E''$). The possibility of such a spontaneous violation of the spatial symmetry is due to the character of the temperature dependence of the absorption coefficient $\alpha(T)$. The colder sections of the rod are not heated because less heat is released in them. The stability of the inhomogeneous solutions $\theta = \theta_0(X)$ is investigated by linearizing (1.11):

$$\theta=\theta_0(X)+\theta_1(X)e^{-\varepsilon\tau},$$
$$\mu d^2\theta_1/dX^2=[-\varepsilon+V(X)]\theta_1, \tag{1.12}$$
$$V(X)=\left.\frac{dF}{d\theta}\right|_{\theta=\theta_0(X)}=-\left.\frac{d^2U}{d\theta^2}\right|_{\theta=\theta_0(X)}.$$

Equation (1.12) can interpreted as a one-dimensional Schrödinger equation with a potential $V(X)$ and an energy

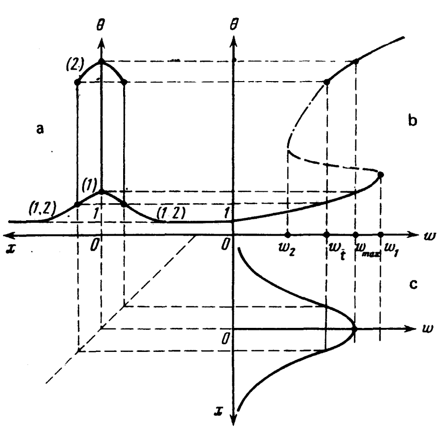

FIG. 3. Scheme for determining the temperature profiles: a) two profiles (1) and (2) of the temperature $\theta_{(1),(2)}$ which are possible at $w_t < w_{max} < w_1$; b) hysteresis dependence of the temperature $\theta(w)$ on the light intensity for an unbounded beam (plane wave); c) light-intensity profile $w = w(X)$, $w_{max} = w(0)$.

ε. Instability corresponds to the presence of discrete negative-energy levels. They exist provided that the potential well present in the region of the inhomogeneous solutions is not too narrow.[35] The inhomogeneous solutions are therefore unstable in the cases when the temperature change is not small, which are apparently of practical interest.

The last conclusion, however, is incorrect in the important case when

$$w=w_t,\quad E=E_t. \tag{1.13}$$

We are dealing then with a transition-type temperature profile (Fig. 1) that approaches asymptotically, as $X \to \pm\infty$, constant values corresponding to the upper and lower branches of the hysteresis curve. The actual form of the profile can be obtained by substituting the values (1.13) in (1.9).

We ascertain now what takes place with such an inhomogeneous profile when the intensity changes: $w \neq w_t$. It is appropriate to note here the analogy between the general form of the nonstationary equation (1.1) at $w(X) = w =$ const with the equations investigated in the problem of diffusion propagation of chemical threshold reactions in a flame.[28,29] This analogy predicts the existence of switching waves between the lower and upper branches of the hysteresis curves; these waves propagate in the transverse X direction at a constant velocity v and with an invariant temperature profile. For stationary displacement waves, replacing the time τ by the variable $\zeta = \tau - X/v$, we change from (1.11) to the equation

$$\frac{d\theta}{d\zeta}=-F(\theta)+\frac{1}{v^2}\frac{d^2\theta}{d\zeta^2}. \tag{1.14}$$

Apart from the notation and the actual form of the function $F(\theta)$, Eq. (1.14) coincides with Eq. (7.11) in Zhabotinskiĭ's monograph,[29] so that we can use the known results. We indicate only that the front velocity is determined uniquely and depends only on the intensity w. Wave propagation of this type is stable[36] (the unstable solutions are those in the form of switching waves on the unstable section of the hysteresis curve). At $w = w_t$ the front propagation velocity vanishes, $v = 0$, and we obtain the stationary inhomogeneous solutions cited above.

Solutions for a steplike $w(X)$ dependence are obtained by matching at the intensity-discontinuity points the values of the temperature θ and of the heat flux $d\theta/dX$. For one step

$$w(X)=\begin{cases} w^-, & X<0,\\ w^+, & X>0, \quad w^+>w^-\end{cases}$$

the asymptotic values of the temperature $\theta^{\pm} = \theta_{X\to\pm\infty}$ are determined by a condition similar to (1.10)

$$w^{\pm}=b(\theta^{\pm})/a(\theta^{\pm}). \tag{1.15}$$

This corresponds in Fig. 4 to motion along horizontal straight lines with energy levels $E^{\pm} = U(\theta^{\pm})$. The temperature $\theta_0 = \theta|_{X=0}$ is determined by the relation

$$A(\theta_0)=(E^+-E^-)/(w^+-w^-). \tag{1.16}$$

The geometric determination of θ_0 is illustrated with

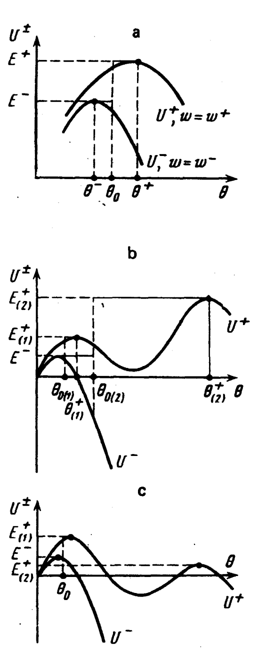

FIG. 4. "Potential curves" for steplide function $u(X)$: a) "matching" of the solutions for two humps; b) hysteresis, the indices (1) and (2) pertain to the two possible solutions; c) absence of hysteresis at $w_2\, w^+\, w_t$, the unique solution corresponds to mixing of two left-hand humps.

the aid of Fig. 4. Corresponding to a certain value of θ_0 is the same value of the kinetic energy for both ($w = w_+$ and $w = w_-$) potential curves. For fixed values of $\theta^\pm$, in view of the monotonic character of $A(\theta)$ [since $dA/d\theta = a(\theta) > 0$], relation (1.16) yields not more than than one value of θ_0, after which the temperature profile is completely determined by (1.9) for both $X<0$ and $X>0$. Hysteresis appears at $w_t < w^+ < w_1$, when the same value of w^+ corresponds to two values of θ^+ and E^+ (Fig. 4b). We note there is no hysteresis in the intensity interval $w_2 < w^+ < w_t$, since no matching is possible at $E = E_2^+ < E^-$ (Fig. 4c) [the right-hand side of (1.16) becomes negative, whereas the left side is always positive]. Other steplike variations of the beam intensity can be treated similarly.

Although the correct form of the temperature profile can be obtained for a smooth beam by replacing $w(X)$ with a series of steps and using relations of the type (1.16), we shall obtain the solution of the problem (1.4), (1.5) by an asymptotic (singular-perturbation) method[37] based on the smallness of the "mass" $\mu \ll 1$. The solution is made up of external expansions that are matched internally by the boundary-layer expansion. The external expansion corresponds to solution of (1.4) and (1.5) in the form of a series

$$\theta^{ext}(X) = \sum_{s=0}^{\infty} \mu^s \theta_s^{ext}(X).$$

In the lowest approximation ($\mu = 0$) it follows from (1.4) that $F = 0$. The corresponding coordinate profile $\theta_0^{ext}(X)$ is obtained by inverting the relation

$$w(X) = b(\theta_0^{ext})/a(\theta_0^{ext}) \qquad (1.17)$$

which is the inverse of (1.10) and (1.15). The temperature profile for the external solutions is thus represented in the assumed approximation by motion along the vertices of the left-side (lower branch of the hysteresis curve of Fig. 3b) and right-hand (upper branch) humps of the potential curves (lines LL and RR in Fig. 1). For smooth solutions confined to the lower branch only [this calls for the condition $w(X) < w_1$] the external solution with (1.17) is already sufficient. At $w_{max} = \max w(X)$, only solutions with jumps between the branches are possible. To construct a solution with a jump it is necessary to resort to the boundary layer (internal expansion), the position of which X_t is generally not known beforehand. We introduce a new coordinate

$$\tilde{x} = (X - X_t)/\mu^{1/2}.$$

After expanding $w(X)$ in a Taylor series in the vicinity of X_t, Eq. (1.4) takes the form

$$\frac{d^2\theta^{BL}}{d\tilde{x}^2} = -\left[w_0 + w_1\mu^{1/2}\tilde{x} + \frac{1}{2!} w_2\mu\tilde{x}^2 + \ldots\right] a(\theta^{BL}) + b(\theta^{BL}), \qquad (1.18)$$

where $w_n = d_n w/dX_n |_{X=X_t}$. The solution of (1.18) is constructed in the form of a series

$$\theta^{BL}(\tilde{x}) = \sum_{s=0}^{\infty} \mu^{s/2} \theta_s^{BL}(\tilde{x}).$$

In the lowest approximation it follows from (1.18) that

$$d^2\theta_0^{BL}/d\tilde{x}^2 = -w_0 a(\theta_0^{BL}) + b(\theta_0^{BL}),$$

which coincides with (1.4) if the substitutions $\mu \to 1$ and $w(X) \to w_0 = w(X_t)$ are made. The corresponding solutions were given above [see (1.9)].

The boundary layer should thus be represented by a section of the horizontal line $E = \text{const}$ (Fig. 1). Our problem reduces now to construction of a solution that consists of motion on the left humps [$X < X_t$ for the increasing section of $w(X)$ or $X > X_t$ for the section where $w(X)$ decreases], a "horizontal" transition from the left hump to the right at $X \approx X_t$, followed by motion over the right humps (at $X > X_t$ or $X < X_t$). It follows from the foregoing that the transition from the left to the right hump is possible only if their heights are equal, $E = E_t$, corresponding to an intensity $w = w_t$. This determines the position of the boundary layer from the condition

$$w(X_t) = w_t \qquad (1.19)$$

For this boundary layer at we arrive at $\tilde{x} \to \pm\infty$ at the vertex of the right and left hump, respectively

$$\theta_0^{BL}(+\infty) = \theta_{0(2)}^{ext}, \quad \theta_0^{BL}(-\infty) = \theta_{0(1)}^{ext},$$

and we use for the external expansion the upper (2) and lower (1) hysteresis branches, respectively. With increasing $|X|$ the deviations of θ_0^{BL} from the indicated asymptotic values decrease exponentially.

The geometric value $w = w_t$ corresponds to an incident-radiation intensity such that the heights of the left and right humps of the potential curve coincide (Fig. 1). Relation (1.6) allows us to reformulate this condition into the requirement that the two shaded areas on Fig. 2 be equal. After determining with the aid of (1.19) the position of the boundary layer, relation (1.9) describes its profile with a characteristic width $\sim(\lambda/H)^{1/2} \ll x_0$. If the last inequality no longer holds or the beam width x_0 approaches the size of the rod, the hysteresis of the temperature profile becomes less pronounced.

Neglecting the small width of the boundary layer, the temperature profile is described by the construction of Fig. 3. We have confined ourselves here to the approximation with independent boundary layers, which is valid if the distance between them exceeds their width. If the maximum intensity over the beam $w_{max} < w_t$, then we have a unique solution that corresponds fully to the lower branch of the hysteresis curve, so that the left-hand edge of the upper branch of the hysteresis curve (dash-dot in Figs. 1 and 3b) is not realized. The solution is also unique at $w_{max} > w_1$, but it consists of a central section corresponding to the upper branch of the hysteresis curve ($w > w_t$), and of a peripheral region determined by the lower branch ($w < w_t$), with a jump between them in the vicinity of $w \approx w_t$. Hysteresis appears in the temperature profile, in accord with the foregoing analysis for a steplike $w(X)$ dependence, only in the range $w_t < w_{max} < w_1$, when at a fixed incident beam we have a smooth profile 1 constructed in accord with the lower branch (Fig. 3a) and a profile 2 with a jump between the branches.

Which of the two possible $\theta(X)$ profiles is established depends on the prior history. If the radiation power $w_{max}(t)$ increases slowly with time to the value $w_{max} \approx w_1$, the profile $\theta(X)$ will be smooth and correspond to the lower branch of the hysteresis curve. In the vicinity of $w_{max} = w_1$ there is produced at the center of the beam a narrow and abrupt temperature spike, which subsequently broadens gradually, even when w_{max} stabilizes, to the stationary position corresponding to condition (1.19). The velocity of the expansion front for broad beams is close to $v = v(w_f)$, where w_f is the local value of the beam intensity in the region of the front, and v is the switching-wave propagation velocity defined by Eq. (1.14). When the indicated stationary position $v_f = v_t$ is approached, the front slows down: $v \to 0$. The hysteresis transition takes place thus not simultaneously over the entire beam cross section, but in a narrow zone—the moving front of the switching wave. Accordingly, the time of the hysteresis transition is determined by the velocity v of the transverse propagation of the switching wave.

The foregoing results are fully applicable also to the case of a plate irradiated by an axisymmetric light beam, provided that the jump defined by the condition (1.19) between the branches of the hysteresis curve does not take place in the immediate vicinity ($\sim(\lambda/H)^{1/2}$) of the beam axis. Indeed, in the considered lowest-order approximation in μ, the additional term $(\mu/r)d\theta/dr$ that appears in the left-hand side of Eq. (1.4) does not enter in either the external or the internal expansion. The anomalously large values of the temperature gradient (in the radial direction), which appear in the narrow boundary layer or in the front of the switching wave (ring), determine essentially the thermoelastic stresses of semiconducting optical materials.[38] A numerical analysis shows that the switching waves and the stationary profiles are stable, and confirms also the indicated character of the kinetics of the hysteresis transition.

2. NONLINEAR INTERFEROMETER

We consider a Fabry-Perot interferometer in which a nonlinear medium is placed. Hysteresis is possible in such such interferometers at practically any type of nonlinearity.[14] Since the hysteresis characteristics are common to various nonlinear interferometers, we confine ourselves, for the sake of argument, to the case of saturation absorption.[15] For a Kerr nonlinearity, and later also for other types of nonlinearity, boundary layers and hysteresis of the light-beam profile were found in Ref. 27 with diffraction of the light taken into account. Diffraction means the mixing of neighboring light tubes that are independent of one another in the geometric-optics approximation. For the analytic treatment we shall find it more convenient to consider another type of mixing, namely spatial diffusion of the nonlinear medium, neglecting at the same time the diffraction of the light. This is justified if the diffusion path during the lifetime τ_0 of the levels that are at resonance with the optical radiation exceeds the characteristic width $\sim(\lambda L)^{1/2}$ of the diffraction spreading, i.e.,

$$D\tau_0 \gg \lambda L,$$

where D is the diffusion coefficient, λ is the wavelength of the light, and L is the interferometer length. The diffusion coefficients in gases and liquids are given in a handbook.[39] Diffusion can take place also in the absence of mechanical motion of the particles (for example in activated solids via interaction of impurity centers).

The kinetic equation for the population difference of the lower and upper levels n is of the form

$$\frac{\partial n}{\partial t} = -\frac{n-n_0}{\tau_0} - BnI + D\Delta n, \quad 0<z<l, \tag{2.1}$$

where B is the Einstein coefficient, I is the light intensity, Δ is the Laplace operator, the term n_0/τ_0 is the difference between the pumping rates to the upper and lower levels, z is the coordinate along the interferometer axis, and l is the thickness of the nonlinear layer. Equations similar to (2.1) were used earlier in laser theory.[40]

Since we are interested here in transverse distribution effects, we average over the longitudinal direction z, which coincides with the beam axis (the validity of the averaging was investigated in detail, e.g., in Refs. 41 and 42, and diffusion mixing extends the region of validity of the averaging). We introduce also the dimensionless quantities

$$\tau = t/\tau_0, \quad X = x/x_0, \quad P = IB\tau_0, \quad w = GB\tau_0,$$

$$\mu = \frac{D\tau_0}{x_0^2}, \quad \theta = \int_0^l \frac{1}{n_0 l} n(z)\,dz, \quad b(\theta) = \theta - 1,$$

where x_0, as before, characterizes the width of the incident light beam, and G is its intensity multiplied by the transmission coefficient of the entrance mirror.

Next, again considering the case of one transverse coordinate X, we reduce (2.1) to the form (1.11), where now

$$F=P\theta-b(\theta). \tag{2.2}$$

To close the equation we use the following connection, which follows from the geometric-optics approximation, between the intensity P inside the interferometer and the intensity w of the incident beam. We assume that this connection is not subject to inertia. This is true in both the stationary and nonstationary regimes, if in the latter case the level lifetime τ_0 exceeds the photon lifetime, which is determined by the figure of merit, in the interferometer. We express the local transmission coefficient of the nonlinear layer in the form (the interferometer is assumed for simplicity to be annular)

$$T=P|_{z=l}/P|_{z=0}=e^{-\xi\theta},\ \xi=\sigma l n_0, \tag{2.3}$$

where σ is the absorption cross section of the transition. Then

$$P=w/[1-2RT^{1/2}\cos\Delta\varphi+R^2T]. \tag{2.4}$$

Here R is the product of the amplitude reflection coefficients of the interferometer mirrors, $\Delta\varphi$ is the dephasing over the interferometer length, due to the deviation between the frequency of the incident signal and the resonant frequency of the interferometer. Expressions (2.3) and (2.4) allow us to express the "force" F in the form (1.4), where

$$a(\theta)=\theta/(1-2R\cos\Delta\varphi e^{-\xi\theta/2}+R^2e^{-\xi\theta}). \tag{2.5}$$

Thus, the difference from the optical thermal breakdown problem considered above, under the assumptions made lies only in the actual form of the function $a(\theta)$. Accordingly, the analysis and the main results of the preceding sections are applicable in their entirety to the case of the nonlinear interferometer. This enables us to find the transverse profile of the population difference $\theta(X)$, from which the intensity of the transmitted light is uniquely determined.

The form of the function $a(\theta)$ that follows from (2.5) is shown in Fig. 5. The character of "potential curves" $U(\theta)$, which can be expressed in terms of a special function (the Eulder dilogarithm) is the same as in Fig. 1. In the stationary regime, the intensity wt corresponding to the transition layer is again determined from the condition that the heights of the left and right bumps be equal, or that the shaded areas in Fig. 5 be equal. The intensity profile is obtained by a construction similar to that indicated in Fig. 3. Hysteresis of the intensity profile is possible under the condition $w_t<w_{\max}<w_1$, where $w_{\max}$ is the maximum intensity of the incident beam on its cross section. Outside this range, the stationary regimes are uniquely determined by the incident beam, and at lower intensities ($w_{\max}<w_t$) the profiles are smooth and correspond to the lower branch, while at higher intensities ($w_{\max}>w_1$) the profile of the central part of the beam is constructed in accord with the upper branch, while that of the peripheral is based on the lower, with a jump between the branches in the region $w\approx w_t$. Just as in the case of optical thermal breakdown, the hysteresis takes place not simultaneously over the entire cross section of the beam, but only in a relatively narrow moving switching front. The switching wave propagation velocity determines in essence the total time of the hysteresis transition. The results are again valid not only for a planar geometry but also for an axisymmetric incident beam.

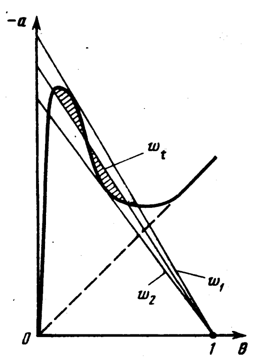

FIG. 5. Typical plot of a (θ) for a nonlinear interferometer.

The presented analysis agrees with the results of the preceding paper,[27] where the position of the boundary layer was determined numerically. Under the conditions of Ref. 27, the calculations led to the relation $w_t\approx w_2$. The very form of the transition-layer profile is not the same, both because of the difference between the mechanism that mixes the light tubes (diffractive in Ref. 27 and diffusive in the present paper) and because the form of the nonlinearity is different.

In the system considered above the longitudinal distribution was not significant, although in the general case it does lead to additional nontrivial singularities in the kinetics. The simplest case here is that of the so-called hybrid optical-bistability schemes. For these schemes, if the time of propagation (retardation) of the light exceeds noticeably the characteristic establishment (relaxation) time there can occur in the feedback circuit periodic and stochastic regimes in the absence of any nonstationarity or noise in the system itself or in the radiation incident on the system.[43] Such regimes were obtained for nonlinear interferometers by Ikeda[44] in the plane-wave approximation.

The possibility of converting stationary incident radiation into pulses after passage through a nonlinear interferometer was pointed out earlier in a number of papers.[15,45,46] These phenomena are typical of multistable systems, for example for an interferometer with saturable absorption and free spectral range,[44] where the stationary solutions corresponding to appreciable sections of the hysteresis curve are unstable. Ikeda's interesting results call, however, for additional verification when it comes to taking into account the transverse structure of the field. An important role is played here by instability of the type of small-scale self-focusing,[27] which lead to a splitting of the beam (or of its central part) in the interferometer into individual filaments. Application of a previously developed procedure[27] to multistable nonlinear interferometers shows that when suitable spatial filtering is produced and the incident beam is stationary, periodic and stochastic time variation of the transmitted beam is possible.[47]

1) In the case of a more complicated mutiloop dependence, the system is called multistable, and is also subject to the effects considered below.

2) The general solutions presented below are actually valid for all boundary conditions, but if one forgoes (1.5) it is necessary to take into account the possibility of additional boundary layers at the ends of the rod. We note that the last term in the right-hand side of (1.2) is written in a form that corresponds to convective heat exchange. Allowance for heat exchange by radiation leads only to a change in the form of the function $b(\theta)$.

3) If the incident radiation is an infinite plane wave, then it can be assumed that $x_0 = (\lambda/H)^{1/2}$ and $\mu = 1$.

4) In addition, as seen from Fig. 1, solutions exist also with periodic dependences of the temperature on the coordinate X, and also solutions that are not bounded as $|X| \to \infty$. They can be disregarded here, since they do not satisfy the boundary conditions (1.5).

1. N. N. Bogolyubov and Yu. A. Mitropol'skiĭ, Asymptoticheskie metody v teorii nelineinykh kolebanii (Asymptotic Method in the Theory of Nonlinear Oscillations), Nauka, 1974 [Gordon & Breach, 1963].
2. V. N. Lugovoĭ, Radiotkh. Élektron. 6, 1700 (1961).
3. W. E. Lamb, jr., Phys. Rev. 134, 1429 (1961).
4. V. S. Letokhov and V. P. Chebotaev, Printsipy nelineĭnoĭ lazernoĭ spektroskopii (Nonlinear Laser Spectroscopy), Nauka, 1975 [Springer, 1977].
5. V. P. Silin, Zh. Eksp. Teor. Fiz. 53, 1662 (1967) [Sov. Phys. JETP 26, 955 (1968)].
6. B. B. Boĭko, I. Z. Dzhilavdari, and N. S. Petrov, Zh. Prikl. Spektr. 23, 888 (1975); 441 (1978).
7. A. E. Kaplan, Pis'ma Zh. Eksp. Teor. Fiz. 24, 132 (1976) [JETP Lett. 24, 114 (1976)]; Zh. Eksp. Teor. Fiz. 72, 1710 (1977) [Sov. Phys. JETP 45, 896 (1977)].
8. V. S. Butylkin, A. E. Kaplan, Yu. G. Khronopulo, and E. I. Yakubovich, Rezonansnye vzaimodeĭstviya sveta s veshchestvom (Resonant Interaction of Light with Matter), Nauka, 1977.
9. N. N. Rozanov, Pis'ma v Zh. Tekh. Fiz. 3, 583 (1977); 4, 74 (1978) [Sov. Tech. Phys. Lett. 3, 239 (1977); 4, 30 (1978)].
10. A. A. Kolokolov and A. I. Sukov, Izv. vyssh. ucheb. zaved. Fizika 31, 1309 (1978).
11. K. Sauer and L. M. Gorbunov, Fiz. Plazmy 3, 1302 (1977) [Sov. J. Plasma Phys. 3, 724 (1977)].
12. L. A. Bol'shov and V. P. Reshetin, Kvant. Elektron. (Moscow) 7, 538 (1980) [Sov. J. Quantum Electron. 10, 305 (1980)].
13. É. M. Épshteĭn, Zh. Tekh. Fiz. 48, 1733 (1978) [Sov. Phys. Tech. Phys. 23, 983 (1978)].
14. V. N. Lugovoĭ, Kvant. Elektron. (Moscow) 6, 2053 (1979) [Sov. J. Quantum Electron. 9, 1207 (1979)].
15. A. Szöke, V. Danen, J. Goldhar, and N. A. Kurnit, Appl. Phys. Lett. 15, 376 (1969).
16. V. N. Lugovoĭ, Zh. Eksp. Teor. Fiz. 76, 1943 (1979) [Sov. Phys. JETP 49, 985 (1979)]; Phys. Lett. 69A, 402 (1979).
17. D. A. Miller and S. D. Smith, Opt. Commun. 31, 101 (1979).
18. I. Sh. Averbukh, V. A. Kovarsky, and N. F. Perelman, Phys. Lett. 74A, 36 (1979).
19. L. Lugiato, Nuovo Cimento B50, 89 (1979).
20. A. Schenzle and H. Brand, Opt. Commun. 31, 401 (1979).
21. J. Chrostowski and A. Zardecki, Opt. Commun. 39, 230 (1979).
22. F. A. Horf and P. Meystre, Opt. Commun. 29, 235 (1979).
23. K. Kondo, M. Mabuchi, and H. Hasegawa, Opt. Commun. 32, 136 (1980).
24. S. L. McCall, Phys. Rev. A9, 1515 (1974).
25. H. H. Rozanov, Opt. Spektrosk. 47, 606 (1979) [Opt. Spectrosc. (USSR) 47, 335 (1979)].
26. A. A. Kolokolov and A. I. Sukov, Izv. vyssh. ucheb. zav. Radiofizika 31, 1459 (1978).
27. N. N. Rozanov, and V. E. Semenov, Opt. Spektrosk. 48, 108 (1980) [Opt. Spectrosc. (USSR) 48, 59 (1980)].
28. D. A. Frank-Kamenetskiĭ, Diffuziya i teploperedacha v khimicheskoĭ kinetike (Diffusion and Heat Transfer in Chemical Kinetics), Nauka, 1970.
29. A. M. Zhabotinskiĭ, Kontsentratsionnye avtokolebaniya (Concentration Self-Oscillations), Nauka, 1974.
30. G. Nicolis and I. Prigogine, Self-Organization in Non-Equilibrium Systems, Wiley, 1977.
31. V. A. Vasil'ev and Yu. M. Romanovskiĭ, Usp. Fiz. Nauk 128, 625 (1979) [Sov. Phys. Usp. 22, 615 (1979)].
32. A. F. Volkov and Sh. M. Kogan, Usp. Fiz. Nauk 96, 633 (1968) [Sov. Phys. Usp. 11, 881 (1969)].
33. N. N. Rozanov, Pis'ma v Zh. Tekh. Fiz. 6, 778 (1980) [Sov. Tech. Phys. Lett. 6, 335 (1980).
34. L. D. Landau and E. M. Lifshitz, Mekhanika (Mechanics), Nauka, 1965 [Pergamon, 1978].
35. L. D. Landau and E. M. Lifshitz, Kvantovaya Mekhanika (Quantum Mechanics, Nonrelativistic Theory), Nauka, 1974 [Pergamon].
36. A. N. Kolmogorov, I. G. Petrovskiĭ, and N. S. Piskunov, Byull. MGU, ser. A, 1, 6 (1937).
37. A. B. Vasil'eva and V. F. Butuzov, Asimptoticheskie razlozheniya resheniĭ singulyarno vosmushchennykh uravneniĭ (Asymptotic Expansions of the Solutions of Singularly Perturbed Equations), Nauka, 1973.
38. V. V. Reznichenko and Vl. N. Smirnov, Zh. Tekh. Fiz. 49, 633 (1979) [Sov. Phys. Tech. Phys. 24, 362 (1979)].
39. N. B. Vargaftik, Spravochnik po teplofizicheskim svoĭstvam gazov i zhidkosteĭ (Handbook of Thermophysical Properties of Gases and Liquids), Fizmatgiz, 1963.
40. V. S. Mashkevich, Kineticheskaya teoriya lazerov (Kinetic Theory of Lasers), Nauka, 1971.
41. R. Bonifacio and L. A. Lugiato, Lett. Nuovo Cimento 31, 505, 517 (1978).
42. P. Meystre, Opt. Commun. 26, 277 (1978).
43. N. N. Rozanov, Pis'ma v Zh. Tekh. Fiz. 6, 173 (1980) [Sov. Tech. Phys. Lett. 6, 77 (1980)].
44. K. Ikeda, Opt. Commun. 30, 257 (1979).
45. V. N. Lugovoi, Opt. Acta 24, 743 (1977).
46. R. Bonifacio, M. Gronchi, and L. A. Lugiato, Opt. Commun. 30, 129 (1979).
47. N. N. Rozanov, V. E. Semenov, and G. V. Khodova, Abstracts, 10th All-Union Conf. on Coherent and Nonlinear Optics, Kiev, 1980.

Translated by J. G. Adashko